DOI: 10.1002/ejic.200800756

Isostructural Potassium and Thallium Salts of Sterically Crowded Thio- and Selenophenols: A Structural and Computational Study

Denis Bubrin[a] and Mark Niemeyer*[b]

Keywords: Pi interactions / Potassium / S ligands / Se ligands / Terphenyl ligands / Thallium

Because of their similar cationic radii, potassium and thallium(I) compounds are usually regarded as closely related. Homologous molecular species containing either K^+ or Tl^+ are very rare, however. We have synthesized potassium and thallium salts MEAr* [M, E = K, S (**2a**); K, Se (**2b**); Tl, S (**3a**); Tl, Se (**3b**); Ar* = 2,6-$Trip_2C_6H_3$, Trip = 2,4,6-$i Pr_3C_6H_2$] derived from terphenyl-substituted thio- and selenophenols. In the solid-state structures of dimeric **2a**, **2b**, **3a**, and **3b** additional metal-η^n–π-arene interactions to the flanking arms of the terphenyl substituents of different hapticity *n* are observed. Remarkably, the homologous potassium and thallium complexes **2b** and **3b** crystallize in isomorphous cells. For **2a**, **3a**, and model complexes of the composition METph (Tph = C_6H_4-2-Trip) the nature of the M–E and M···C(arene) bonding was studied by density functional theory calculations.

Introduction

Thallium, the heaviest element in group 13, shows similarities to other elements in the Periodic Table, in particular, the alkali metals, Ag, Hg, and Pb,[1] an observation that led Dumas to describe it as the "duckbill platypus among elements."[2,3] For example, compounds of monovalent thallium can be compared to those of potassium (e.g. hydroxides, carbonates, sulfates) or silver (e.g. oxides, sulfides, halides).[4] Furthermore, the similar ionic radii of Tl^+ and K^+ (1.64 Å vs. 1.55 Å for sixfold coordination)[5–7] together with the higher affinity to enzymatic sites of the former are responsible for the easy incorporation and the high toxicity of soluble thallium species. For this reason, there has been much interest in the use of Tl^+ as a probe in biochemical systems since thallium is much more easily detectable by diffraction methods[8] or NMR spectroscopy.[9]

Although some simple thallium or potassium salts crystallize isotypically,[10] this is not the case for molecular organometallic or coordination compounds. Thus, thallium(I) cations often show exceedingly low coordination numbers leaving a large part of the coordination sphere seemingly unoccupied.[11,12] By using an extremely bulky terphenyl ligand it was even possible to stabilize an arylthallium(I) compound with a quasi-one-coordinate metal atom.[13] By contrast, potassium cations always have their coordination sphere covered as completely and as symmetrically as possible, optimizing the Coulomb energy and inter-ligand interactions. These differences are usually attributed to the relativistically contracted valence shell and the stereochemically active $6s^2$ lone pair of electrons in the former.[7] The limited number of structurally characterized K^I or Tl^I species with the same composition (Table 1) most probably originates from the higher tendency of K^+ to coordinate additional solvent molecules. In the absence of coordinating solvents the mainly ionic potassium compounds usually aggregate by bridging donor atoms, intermolecular metal···arene interactions, or agostic metal···C–H contacts in order to optimize the Coulomb energy.[23] Similar factors contribute to the aggregation of thallium compounds[12] which are considered less ionic, however. In addition, the aggregation behavior is influenced by the presence of weak attractive, thallophilic[11] interactions between Tl^I centers.

Very recently, we have reported the synthesis and structural characterization of a series of potassium and thallium salts derived from biphenyl- or terphenyl-substituted triazenes.[22] Those complexes appear to be the first examples of isostructural molecular species reported for these elements. In this paper, we describe the synthesis and characterization of thallium thiolates and selenolates substituted by a sterically crowded *m*-terphenyl substituent. Although, the related potassium derivatives have been known for some time[24] we have prepared and structurally authenticated further derivatives in order to allow a better comparison with the corresponding thallium salts.

[a] Institut für Anorganische Chemie, Universität Stuttgart, Pfaffenwaldring 55, 70569 Stuttgart, Germany
[b] Institut für Anorganische und Analytische Chemie, Johannes-Gutenberg-Universität Mainz, Duesbergweg 10–14, 55128 Mainz, Germany
Fax: +49-6131-39-25407
E-mail: niemeyer@uni-mainz.de

Supporting information for this article is available on the WWW under http://www.eurjic.org or from the author.

Table 1. Selected structural data [Å] for homologous K and Tl compounds.[a]

Compound	Description	Intramolecular distances	Intermolecular distances	Ref.
KCp	polymeric structure of interconnected chains	K–C {3.05}	K···C > 3.33 K···K > 4.45	[14]
TlCp	polymeric chain structure	Tl–C {2.99}	Tl···C > 3.89 Tl···Tl > 3.94	[15]
$KN(SiMe_3)_2$	associated dimers	K–N {2.79} K···C > 3.34	K···C > 3.30 K···K > 5.51	[16]
$TlN(SiMe_3)_2$	dimeric	Tl–N 2.58 Tl···C > 3.50	Tl···C > 4.03 Tl···Tl > 3.94	[17]
KOMe	double-layered structure	K–O {2.73} K···K > 3.68		[18]
TlOMe[b]	tetrameric	Tl···Tl > 3.84		[19]
K(18-cr-6) ClO_4	K in O_6 plane	K–O {2.82} K–O_4Cl 2.75	K–O_4Cl 2.85	[20]
Tl(18-cr-6) ClO_4	Tl out of O_6 plane	Tl–O {2.93} Tl–O_4Cl 2.94	Tl–O_4Cl 3.05	[7]
KN_3Tph_2[c]	monomeric	K–N {2.72} K···C {3.36}		[21]
TlN_3Tph_2[c]	monomeric	Tl–N {2.59} Tl···C {3.46}		[22]

[a] Average values in braces. [b] Only positions of Tl atoms were determined. [c] Tph = C_6H_4-2-Trip with Trip = 2,4,6-iPr$_3$$C_6H_2$.

Results and Discussion

The thallium and potassium thio- and selenophenolates are accessible in heptane as the solvent by metalation of the thiols and selenols Ar*SH or Ar*SeH [Ar* = 2,6-Trip$_2$$C_6H_3$; Trip = 2,4,6-$iPr_3$$C_6H_2$] with either thallium ethoxide or potassium metal (Scheme 1). Crystallization from the same solvent afforded the colorless metal thiolates KSAr* (**2a**) and TlSAr* (**3a**) in isolated yields of 94% and 80%, respectively, whereas the colorless metal selenolates KSeAr* (**2b**) and TlSeAr* (**3b**) were obtained as packing complexes with *n*-heptane [(**2b**)$_2$/(**3b**)$_2$·(C_7H_{16})$_{0.5}$] in yields of 97% and 77%, respectively. Since crystals of **3a** proved to be difficult to examine by X-ray crystallography, because of twinning problems, they were converted into the packing complex (**3a**)$_2$·(C_5H_{10})$_3$ by recrystallization from cyclopentane.

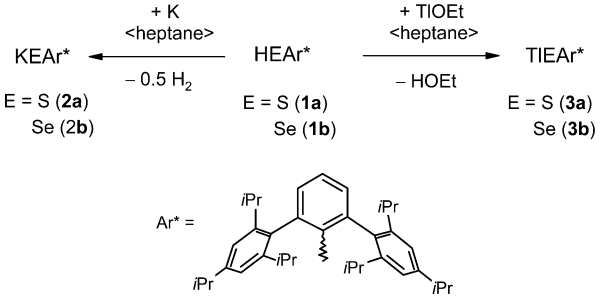

Scheme 1. Synthesis of compounds **2a**,**b** and **3a**,**b**.

In the ^{13}C NMR spectra the almost identical resonances for the i-C_6H_3 carbon atom of δ = 157.4 (**3a**) and 157.0 ppm (**2a**)[24a] for the metal thiolates on one side and δ = 149.2 (**3b**) and 149.4 ppm (**2b**)[24b] for the metal selenolates on the other side indicate a similar charge balance in the thallium and potassium derivatives. Unfortunately, it was not possible to detect a ^{77}Se NMR signal for **3b** and to compare it with the corresponding resonance of δ = 179 ppm for **2b**.

Compounds **2a**, **2b**, **3a**, and **3b** were examined by X-ray crystallography. Their molecular structures are shown in Figures 1, 2, and 3 (for a molecular plot of **2b** and additional projections of all compounds, see the Supporting Information), whereas selected structural parameters are given in Figure 1 and Table 2. All compounds crystallize as dimers with M_2E_2 cores. As indicated by the folding angles

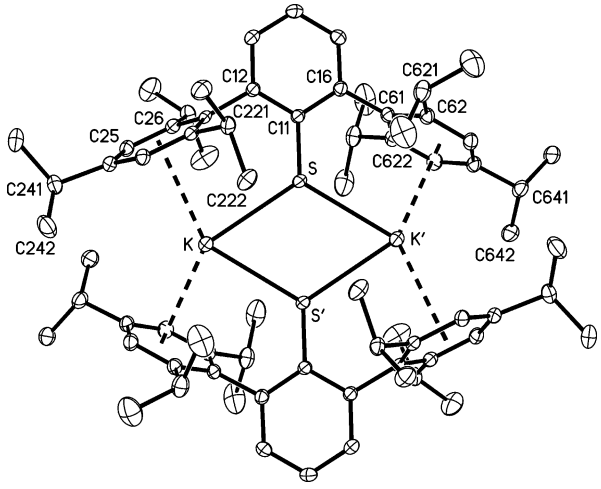

Figure 1. Molecular structure of **2a** with thermal ellipsoids set to 30% probability. Hydrogen atoms have been omitted for clarity. Selected bond lengths [Å] and angles [°]: K–S 3.0529(8), K–S′ 3.0566(6), S–C11 1.7488(15), S–K–S′ 65.012(17), K–S–K′ 114.948(18), K···C21 3.4076(15), K···C22 3.3463(15), K···C23 3.3258(15), K···C24 3.3909(15), K···C25 3.3914(16), K···C26 3.4052(16), K···C61′ 3.4719(16), K···C62′ 3.3973(17), K···C63′ 3.2996(18), K···C64′ 3.2930(17), K···C65′ 3.3496(17), K···C66′ 3.4464(16).

along the E···E vector of 179.4° (**2a**), 177.6° (**2b**), 171.7° (**3a**), and 179.6° (**3b**), the four-membered rings are almost planar. Compounds **2b**, **3a**, and **3b** crystallize without im-

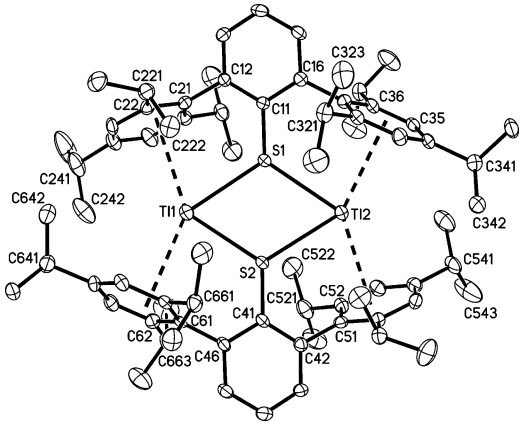

Figure 2. Molecular structure of **3a** with thermal ellipsoids set to 30% probability. Hydrogen atoms and cocrystallized solvent molecules have been omitted for clarity. For selected bond parameters, see Table 2.

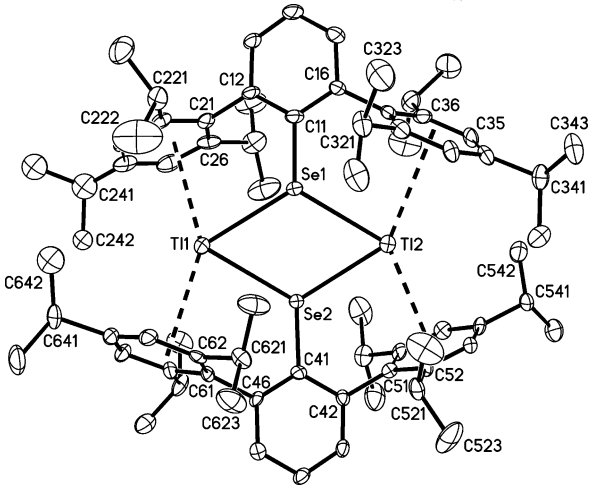

Figure 3. Molecular structure of **3b** with thermal ellipsoids set to 30% probability. Hydrogen atoms and cocrystallized solvent molecules have been omitted for clarity. For selected bond parameters, see Table 2.

Table 2. Selected bond lengths [Å] and angles [°] for compounds **2a**,**b** and **3a**,**b**.[a,b]

	2b (M = K, E = Se)	**3a** (M = Tl, E = S)	**3b** (M = Tl, E = Se)
M1–E1	3.1516(7)	2.9064(13)	2.9827(9)
M1–E2	3.1750(7)	2.8510(13)	3.0160(8)
M2–E1	3.1553(8)	2.8769(13)	2.9597(9)
M2–E2	3.1842(8) {3.167}	2.9020(12) {2.884}	2.9731(9) {2.983}
E1–M1–E2	64.185(14)	66.96(4)	65.70(2)
E1–M2–E2	64.039(15)	66.68(4)	66.53(2)
M1–E1–M2	116.640(19)	112.27(4)	114.57(3)
M1–E2–M2	115.132(19)	113.17(4)	113.19(3)
M1···C21	3.457(3)	3.456(4)	3.432(7)
M1···C22	3.457(3)	3.457(5)	3.521(7)
M1···C23	3.374(3)	3.543(5)	3.576(7)
M1···C24	3.306(3)	3.631(5)	3.530(7)
M1···C25	3.268(3)	3.598(5)	3.437(8)
M1···C26	3.350(3) {3.369}	3.554(5) {3.540}	3.408(8) {3.484}
M1···C61	3.449(3)	3.493(4)	3.453(7)
M1···C62	3.333(3)	3.504(5)	3.389(7)
M1···C63	3.251(3)	3.615(5)	3.413(8)
M1···C64	3.313(3)	3.711(5)	3.541(8)
M1···C65	3.363(3)	3.651(5)	3.582(8)
M1···C66	3.445(3) {3.359}	3.565(4) {3.590}	3.518(8) {3.483}
M2···C31	3.637(3)	3.434(4)	3.624(7)
M2···C32	3.757(3)	3.428(4)	3.775(8)
M2···C33	3.678(3)	3.464(5)	3.816(8)
M2···C34	3.516(3)	3.514(4)	3.758(8)
M2···C35	3.362(3)	3.504(4)	3.607(8)
M2···C36	3.432(3) {3.564}	3.470(5) {3.469}	3.544(7) {3.687}
M2···C51	3.630(3)	3.407(4)	3.567(7)
M2···C52	3.384(3)	3.415(5)	3.480(7)
M2···C53	3.304(3)	3.486(5)	3.523(6)
M2···C54	3.472(3)	3.564(5)	3.694(6)
M2···C55	3.670(3)	3.547(5)	3.754(7)
M2···C56	3.760(3) {3.537}	3.470(5) {3.482}	3.745(7) {3.627}
$\eta^n/\eta^m/\eta^o/\eta^p$	$\eta^5/\eta^5/\eta^4/\eta^4$	$\eta^5/\eta^5/\eta^6/\eta^5$	$\eta^5/\eta^5/\eta^5/\eta^5$
M1···X6/M1···X*n*	3.069/3.062	3.255/3.248	3.193/3.184
M1···X6′/M1···X*m*	3.056/3.050	3.307/3.294	3.194/3.183
M2···X6′′/M2···X*o*	3.283/3.251	3.176	3.411/3.393
M2···X6′′′/M2···X*p*	3.255/3.210	3.190/3.185	3.351/3.332
X6···M1···X6′	145.7	131.8	141.0
X6′′···M2···X6′′′	143.2	134.0	135.3

[a] Average values are given in braces. [b] X6, X6′, X6′′, X6′′′: centroids of the C21→C26, C61→C66, C31→C36, and C51→C56 rings.

posed symmetry, whereas **2a** contains a C_2 axis orthogonal to the K_2S_2 ring. The degradation of symmetry can be traced back to the cocrystallized solvent, one half of a disordered *n*-heptane molecule in isomorphous **2b** and **3b** and three cyclopentane molecules in **3a**. Notably, there are no close interactions between the solvents of crystallization and the chalcogenolate dimers. Similar "asymmetric" solvates with the composition $(KSAr^*)_2$·(toluene), $(KSeAr^*)_2$·(toluene), and $(KSeAr^*)_2$·(OEt_2) have been structurally characterized before.[24] With average bond lengths of 3.0548(8) Å and 3.167(7) Å, the K–S and K–Se distances are almost identical to the distances of the known solvates and reflect the difference between the covalent radii of sulfur (1.02 Å) and selenium (1.17 Å),[5] the average K–Se distance being slightly shorter than expected. A similar trend is observed for the thallium compounds with mean Tl–S and Tl–Se distances of 2.879 Å and 2.983 Å. Notably, these values are 16% shorter than the corresponding distances in the potassium derivatives. The former values may be compared with those in the oligomeric and polymeric thiolates $[Tl_7(SPh)_6^+][Tl_5(SPh)_6^-]$ (2.93 Å for cn_{Tl} = 3; 3.22 Å for cn_{Tl} = 4), $[Tl_8(StBu)_8]$ (2.90 Å; 3.12 Å), and $[\{Tl(SCH_2Ph)\}_\infty]$ (2.90 Å) that contain three- or four-coordinate metal atoms.[25] Whereas structurally characterized compounds with the composition TlSeR have not been reported yet, a couple of species with Tl–Se and Se–C bonds are known. The average Tl–Se bond of 2.983 Å in **3b** is considerably shorter than the distances in the selenoether complex $[Tl\{MeSe(CH_2)_3SeMe\}][PF_6]$ (3.39 Å)[26a] and the diselenolate $[AsPh_4]_2[Tl_2(Se_2C{=}C(CN)_2)_2]$ (3.14 Å),[26b] which show higher coordination numbers of 12 and 4 on the thallium atom, respectively.

Besides their σ-donor free nature, the most interesting feature in the solid-state structures of **2a**,**b** and **3a**,**b** is the presence of additional metal···π-arene contacts to the flanking aryl groups that provide steric and electronic saturation of the metal cations. In **2a**, the metal ion interacts with the Trip rings of the terphenyl substituents in an η^6/η^5 fashion with K···C distances in the ranges 3.3258(15)–3.4076(15) Å (C21→C26) and 3.2930(17)–3.4464(16) Å (C62′→C66′). The propensity of the potassium atom to interact with aromatic groups is now well documented.[23] The mean K···centroid distance of 3.07 Å to the π-bonded Trip arene rings is unexceptional.[27] It should be noted that the assignment of the hapticity of the metal···π-arene interactions in the compounds discussed in this paper is based on the evaluation of the shortest metal···centroid separation. Alternatively, the smallest angle between the M···centroid vector and the normal of the arene plane may be used to determine the best description. To allow a better comparison, Table 2 not only shows the assigned M···centroid (X_n/X_m/X_o/X_p) distances but also the distances to the center (X6/X6′/X6′′/X6′′′) of the coordinated arene rings (C21→C26/C61→C66/C31→C36/C51→C56). In the potassium selenolate **2b**, the potassium···π-arene interactions are best described as being η^5/η^5 for K1 and η^4/η^4 for K2 with notably longer K···C separations for the latter. The K···C distances considered to be bonding are in the ranges 3.251(3)–3.457(3) Å (C21, C23→C26, C62→C66) for K1 and 3.304(3)–3.637(3) Å (C31, C34→C36, C51→C54) for K2 with corresponding K···centroid (X6/X6′ and X6′′/X6′′′) separations of 3.06/3.07 Å and 3.28/3.26 Å, respectively.

In the thallium thiolate **3a**, the thallium···π-arene interactions may be classified as η^5/η^5 for Tl1 and η^6/η^5 for Tl2 with Tl···C distances in the ranges 3.456(4)–3.651(5) Å (C21→C23, C25, C26, C61→C63, C65, C66) and 3.407(4)–3.547(5) Å (C31→C36, C51→C54, C56) and corresponding Tl···centroid (X6/X6′ and X6′′/X6′′′) separations of 3.26/3.31 Å and 3.18/3.19 Å, respectively. The latter values are comparable to the average Tl···centroid distance of 3.17 Å in the recently reported monomeric triazenide complex TlN_3Tph_2 (Tph = C_6H_4-2-Trip) and are close to the typical range of Tl···centroid distances (2.85–3.18 Å)[28] observed for other structurally characterized Tl–π-arene complexes.[29,30] The shortest Tl···arene separations are found in compounds with weakly coordinating anions and electron-rich aromatic rings such as $[Tl(\eta^6\text{-}MesH)_2][B(OTeF_5)_4]$.[29c]

In the thallium selenolate **3b**, the metal···π-arene interactions are best described as being η^5/η^5 for both Tl1 and Tl2 with again longer M···C separations for the latter, similar as in isomorphous **2b**. The Tl···C distances considered to be bonding are in the ranges 3.389(7)–3.541(8) Å (C21, C22, C24→C26, C61→C64, C66) for Tl1 and 3.523(6)–3.745(7) Å (C31, C32, C34→C36, C51→C54, C56) for Tl2 with Tl···centroid (X6/X6′ and X6′′/X6′′′) separations of 3.19/3.19 Å and 3.41/3.35 Å, respectively. Notably, the metal···centroid distances in **2a** and **2b** are shorter by approximately 4% than those present in **3a** and **3b**.

To further understand the bonding situation in the potassium thio- and selenophenolates **2a/b** with weaker K–S/Se but stronger K···arene bonding on one side and the thallium derivatives **3a/3b** with relatively stronger Tl–S/Se but weaker Tl···arene bonding on the other side, density functional theory (DFT) calculations were undertaken.[31] However, it should be kept in mind that these methods are known to be poor at describing weak interactions that are important in noncovalent bonding, such as the London dispersion (van der Waals attraction), dipole–dipole interaction, or hydrogen bonding. Therefore, we have not used standard functionals like the Becke-type functional B3LYP, but rather Truhlars MPW1B95 functional[32] that was developed and adapted for systems with a high degree of noncovalent bonding. Increasing computer power allows it to study, at least at the DFT level, not only simple model compounds such as the biphenyl-substituted monomeric species METph [M, E = K, S ($\mathbf{4a_M}$); K, Se ($\mathbf{4b_M}$); Tl, S ($\mathbf{5a_M}$); Tl, Se ($\mathbf{5b_M}$)], but also experimentally accessible systems such as the dimeric terphenyl-substituted potassium and thallium thiolates $(MSAr^*)_2$ ($\mathbf{2a_M}$, $\mathbf{3a_M}$) (Scheme 2). Table 3 summarizes selected experimental and DFT-calculated bond parameters for the latter. For the potassium thiolate $(KSAr^*)_2$, there is a reasonably good agreement between the calculated and experimental K–S bond lengths and K···centroid distances with relative differences of only +0.6% and –0.6%, respectively. With a relative error of 0.2% the Tl···centroid distances for the thallium thiolate

$(TlSAr^*)_2$ are well reproduced by the calculations. Less accurate, but still acceptable, results are obtained for the calculated Tl–S bond lengths that are overestimated by +1.4%.

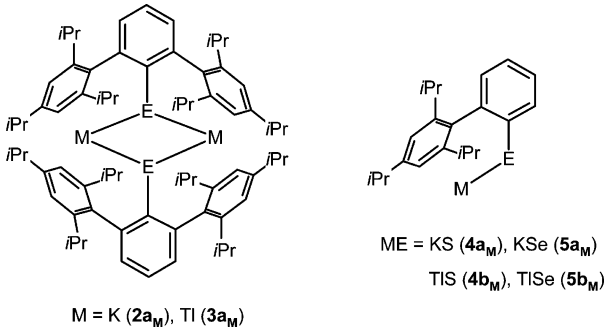

Scheme 2. DFT-calculated model complexes.

Table 3. Comparison of DFT-calculated and experimental bond parameters[a] for the $(MSAr^*)_2$ complexes.

	$(KSAr^*)_2$ exp. $(\mathbf{2a})_2$	$(KSAr^*)_2$ DFT $(\mathbf{2a_M})$	$(TlSAr^*)_2$ exp. $(\mathbf{3a})_2$	$(TlSAr^*)_2$ DFT $(\mathbf{3a_M})$
M–E	3.055	3.074	2.884	2.924
M···C	3.377	3.360	3.520	3.516
M···Cent(η^6)	3.073	3.056	3.232	3.227

[a] Average values.

Further insights into the different bonding situation in **2a/b** and **3a/b** are provided by natural bond orbital (NBO) and NPA (natural population analysis) analyses[33b] on the METph model complexes (Table 4). For $\mathbf{4a_M/4b_M}$, the high NPA charge of +0.921/+0.898 on K and the low Wiberg bond orders[33c] of 0.099/0.139 for the K–S/Se bonds are in accordance with the mainly ionic character of these bonds and slightly higher covalent contributions for the selenium derivative. For $\mathbf{5a_M/5b_M}$, a higher degree of covalent bonding is reflected by an NPA charge of +0.658/+0.607 on Tl and considerably higher Wiberg bond orders of 0.465 and 0.548 for the Tl–S and Tl–Se bonds, respectively. A similar trend is observed for the M···C bonding that is much weaker, however, with smaller Wiberg bond orders of 0.033/0.035 {Σ(K···C)} and 0.126/0.126 {Σ(Tl···C)}. The nevertheless shorter K···C distances are a result of stronger Coulomb contributions as reflected by the different NPA charges on K or Tl on one side and the π-bonded Trip arene rings (average total charges: $C_6H_2iPr_3$ ring, –0.050 {$\mathbf{4a_M}$}, –0.053 {$\mathbf{4b_M}$}, +0.037 {$\mathbf{5a_M}$}, +0.039 {$\mathbf{5b_M}$}; C_6H_2 fragment, –0.173 {$\mathbf{4a_M}$}, –0.171 {$\mathbf{4b_M}$}, –0.112 {$\mathbf{5a_M}$}, –0.107 {$\mathbf{5b_M}$}) on the other side. A close examination of possible interactions between filled (donor) NBOs and empty (acceptor) NBOs by second-order perturbation theory reveals no significant charge delocalization from the lone pair on Tl (with 97.9% *s*-character for both $\mathbf{5a_M}$ and $\mathbf{5b_M}$) to suitable ligand-centered acceptor orbitals.

Table 4. DFT-calculated bond lengths [Å], NPA charges (q), and Wiberg bond orders (BO) for the model complexes $\mathbf{4a_M}$, $\mathbf{4b_M}$, $\mathbf{5a_M}$, and $\mathbf{5b_M}$.

	KSTph $(\mathbf{4a_M})$	KSeTph $(\mathbf{4b_M})$	TlSTph $(\mathbf{5a_M})$	TlSeTph $(\mathbf{5b_M})$
M–E	2.955	3.022	2.670	2.769
av. M···C	3.103	3.084	3.244	3.237
M···Cent(η^6)	2.769	2.748	2.931	2.936
q_M	0.921	0.898	0.658	0.607
q_E	–0.559	–0.513	–0.454	–0.377
q_{C6H4}	–0.313	–0.332	–0.241	–0.269
q_{C6H2}	–0.173	–0.171	–0.112	–0.107
q_{Trip}	0.124	0.118	0.149	0.147
$BO_{M–E}$	0.099	0.139	0.465	0.548
$\Sigma BO_{M–C}$	0.033	0.035	0.126	0.126

Conclusions

We have used sterically crowded thio- and selenophenolate ligands to stabilize dimeric, unsolvated complexes of potassium and thallium. Remarkably, two of those homologous complexes crystallize in isomorphous cells and represent rare examples of molecular thallium and potassium compounds with such behavior. The different nature of the M–E and M···C(arene) bonding was studied by density functional theory calculations that show a higher degree of covalence for the thallium compounds and no significant influence from the lone pair on Tl.

Experimental and Computational Section

General Procedures: All manipulations were performed by using standard Schlenk techniques under purified argon, and solvents were freshly distilled from Na wire or $LiAlH_4$. The ligand precursors and potassium salts Ar*SH, Ar*SeH, KSAr*, and KSeAr* were synthesized as described previously.[24] NMR spectra were recorded with Bruker AC250 or AM400 instruments and referenced to solvent resonances. IR spectra (Nujol mull, CsBr plates) were obtained in the range 4000–200 cm^{-1} with a Perkin–Elmer paragon 1000 PC spectrometer. Melting points were determined under argon in sealed glass tubes.

KSAr* (2a): Colorless crystals of the solvent-free complex were obtained from *n*-heptane at –15 °C. Yield 94%. M.p. 282–284 °C. $C_{36}H_{49}KS$ (552.91): calcd. C 78.20, H 8.93; found C 78.46, H 8.90. ^1H NMR, ^{13}C NMR, and IR data, with exception of solvent resonances, are in agreement with previously reported values for the packing complex $\mathbf{2a}\cdot(C_7H_8)$.[24a]

KSeAr*·$(C_7H_{16})_{0.5}$ [2b·$(C_7H_{16})_{0.5}$]: Colorless crystals of the packing complex were obtained by crystallization of **2a** from *n*-heptane at –15 °C. Yield 97%. M.p. 244–245 °C (dec.). Owing to the lability of the cocrystallized solvent, satisfactory elemental analytical data could not be obtained. ^{77}Se NMR (47.709 MHz, C_6D_6): δ = 179 ppm. ^1H NMR, ^{13}C NMR, and IR data, with exception of solvent resonances, are in agreement with previously reported values for the packing complex $\mathbf{2b}\cdot(C_7H_8)$.[24b]

TlSAr* (3a): To a stirred solution of Ar*SH (1.02 g, 2 mmol) in *n*-heptane (50 mL) was added TlOEt (0.16 mL, 2.0 mmol). The mixture was stirred in the dark for another 24 h, after which all volatile materials were removed under reduced pressure. Another 30 mL of *n*-heptane was added to the remaining solid, and the supernatant liquid was separated by centrifugation from insoluble components (mainly Tl metal). The resulting green solution was reduced to about 15 mL and stored at –15 °C overnight to give colorless crystals of **3a**. Yield: 1.14 g (1.60 mmol, 80%). M.p. 240 °C (dec.). ^1H

NMR (250.133 MHz, C_6D_6): δ = 1.18 [d, $^3J_{HH}$ = 7.5 Hz, 12 H, *o*-CH(CH_3)$_2$], 1.26 [d, $^3J_{HH}$ = 7.5 Hz, 12 H, *p*-CH(CH_3)$_2$], 1.38 [d, $^3J_{HH}$ = 7.5 Hz, 12 H, *o*-CH(CH_3)$_2$], 2.89 [sept, $^3J_{HH}$ = 7.5 Hz, 2 H, *p*-C*H*(CH$_3$)$_2$], 3.19 [sept, $^3J_{HH}$ = 7.5 Hz, 4 H, *o*-C*H*(CH$_3$)$_2$], 6.92–7.26 (m, 7 H, *m*-Trip, *m*/*p*-C_6H_3) ppm. ^{13}C NMR (62.896 MHz, C_6D_6): δ = 24.7 [*o*-CH(*C*H$_3$)$_2$], 24.8 [*o*-CH(*C*H$_3$)$_2$], 25.4 [*p*-CH(*C*H$_3$)$_2$], 31.2 [*o*-*C*H(CH$_3$)$_2$], 34.9 [*p*-*C*H(CH$_3$)$_2$], 120.5 (*p*-C_6H_3), 121.9 (*m*-Trip), 128.8 (*m*-C_6H_3), 141.7 (*o*-C_6H_3) 144.5 (*i*-Trip), 146.9 (*p*-Trip), 148.6 (*o*-Trip), 157.4 (*i*-C_6H_3) ppm. IR (Nujol): $\tilde{\nu}$ = 1600 (m), 1564 (s), 1313 (s), 1258 (m), 1244 (m), 1233 (m), 1169 (s), 1114 (m), 1100 (m), 1068 (w), 1048 (s), 1003 (w), 942 (m), 922 (m), 879 (s), 850 (sh), 798 (m), 784 (sh), 777 (m), 742 (sh), 650 (s), 608 (m), 588 (m), 524 (s), 415 (m), 366 (s), 342 (w) cm^{-1}. $C_{36}H_{49}STl$ (718.23): calcd. C 60.20, H 6.88; found C 59.12, H 6.80.

TlSeAr* (3b): The synthesis was accomplished in a similar manner to the preparation of **3a** with use of Ar*SeH (1.52 g, 2 mmol). Yield 1.16 g (1.54 mmol, 77%) as colorless crystals. M.p. 265 °C (dec.) ^{1}H NMR (250.133 MHz, C_6D_6): δ = 1.11 [d, $^3J_{HH}$ = 7.5 Hz, 12 H, *o*-CH(CH_3)$_2$], 1.30 [d, $^3J_{HH}$ = 7.5 Hz, 12 H, *p*-CH(CH_3)$_2$], 1.38 [d, $^3J_{HH}$ = 7.5 Hz, 12 H, *o*-CH(CH_3)$_2$], 2.84 [sept, $^3J_{HH}$ = 7.5 Hz, 2 H, *p*-C*H*(CH$_3$)$_2$], 2.98 [sept, $^3J_{HH}$ = 7.5 Hz, 4 H, *o*-C*H*(CH$_3$)$_2$], 6.90–7.18 (m, 7 H, *m*-Trip, *m*/*p*-C_6H_3) ppm. ^{13}C NMR (62.896 MHz, C_6D_6): δ = 24.4 [*p*-CH(*C*H$_3$)$_2$], 24.4 [*o*-CH(*C*H$_3$)$_2$], 24.5 [*o*-CH(*C*H$_3$)$_2$], 30.7 [*o*-*C*H(CH$_3$)$_2$], 34.8 [*p*-*C*H(CH$_3$)$_2$], 120.8 (*p*-C_6H_3), 122.7 (*m*-Trip), 126.9 (*m*-C_6H_3), 141.0 (*o*-C_6H_3), 145.3 (*i*-Trip), 147.2 (*p*-Trip), 147.2 (*o*-Trip), 149.2 (*i*-C_6H_3) ppm. IR (Nujol): $\tilde{\nu}$ = 1600 (m), 1563 (s), 1541 (sh), 1314 (s), 1252 (m), 1239 (m), 1168 (m), 1102 (m), 1079 (m), 1068 (m), 1030 (s), 940 (s), 920 (m), 876 (s), 796 (s), 786 (m), 776 (s), 650 (s), 587 (m), 509 (m), 404 (m), 382 (m) cm^{-1}. $(C_{36}H_{49}SeTl)_2(C_7H_{16})_{0.5}$ (1580.26): calcd. C 57.38, H 6.76; found C 57.14, H 6.69.

X-ray Crystallography: X-ray quality crystals were obtained as described above. Crystals were removed from Schlenk tubes and immediately covered with a layer of viscous hydrocarbon oil (Paratone N, Exxon). Suitable crystals were selected, attached to a glass fiber, and instantly placed in a low-temperature N_2 stream.[34a] All data were collected at 173 K with either a Siemens P4 (**2a**, **3b**) or a Bruker Smart Apex II (**2b**, **3a**) diffractometer. Crystal data are given in Table 5. Calculations were performed with the SHELXTL PC 5.03[34b] and SHELXL-97[34c] program systems. The structures were solved by direct methods and refined on F_o^2 by full-matrix least squares. For the thallium complexes an absorption correction was applied by using semiempirical ψ-scans or the multi-scan method. Anisotropic thermal parameters were included for most non-hydrogen atoms, excluding some carbon atoms in disordered groups. For **2b**, the methyl carbon atoms of two disordered isopropyl groups were refined with split positions and site occupation factors of 0.50 (C242, C243/C244, C245, C642/C644). The corresponding C241–C242, C241–C243, C241–C244, C241–C245, C641–C642, and C641–C644 distances were constrained with DFIX commands. The disorder in the cocrystallized heptane molecule was modeled with split positions and SADI restraints for 1,2 and 1,3 distances. For **3a**, the C241–C242 and C241–C243 distances of a *p*-isopropyl group were restrained with SADI commands. All C–C distances in the cocrystallized cyclopentane molecules were constrained with DFIX commands. For **3b**, the methyl carbon atoms of two disordered isopropyl groups were refined with split positions and site occupation factors of 0.50 for C242, C243/C244, C245, and C642/C644. The corresponding C24–C241, C241–C242, C241–C243, C241–C244, C241–C245, C641–C642, and C641–C644 distances were constrained with DFIX commands. The disorder in the cocrystallized heptane molecule was modeled with split positions and SADI restraints for 1,2 and 1,3 distances. Final *R* values are listed in Table 5. Selected bond parameters are given in Figure 1 and Table 3. CCDC-696727 (**2a**), -696728 (**2b**), -696729 (**3a**), and -696730 (**3b**) contain the supplementary crystallographic data for this paper. These data can be obtained free of charge from The Cambridge Crystallographic Data Centre via www.ccdc.cam.ac.uk/data_request/cif.

Table 5. Selected crystallographic data for compounds (**2a**)$_2$, (**2b**)$_2$·$(C_7H_{16})_{0.5}$, (**3a**)$_2$·$(C_5H_{10})_3$, and (**3b**)$_2$·$(C_7H_{16})_{0.5}$.[a]

	(**2a**)$_2$	(**2b**)$_2$·$(C_7H_{16})_{0.5}$	(**3a**)$_2$·$(C_5H_{10})_3$	(**3b**)$_2$·$(C_7H_{16})_{0.5}$
Empirical formula	$C_{72}H_{98}K_2S_2$	$C_{75.50}H_{106}Se_2K_2$	$C_{87}H_{128}S_2Tl_2$	$C_{75.50}H_{106}Se_2Tl_2$
Formula mass	1105.82	1249.73	1646.75	1580.26
Color, habit	colorless, block	colorless, block	colorless, block	pale green, block
Crystal size [mm]	0.90 × 0.70 × 0.55	0.50 × 0.40 × 0.40	0.40 × 0.35 × 0.20	0.50 × 0.40 × 0.40
Crystal system	monoclinic	monoclinic	monoclinic	monoclinic
Space group	*C*2/*c*	*P*2$_1$/*n*	*P*2$_1$/*c*	*P*2$_1$/*n*
a [Å]	15.051(3)	14.9640(5)	15.0246(9)	15.0901(13)
b [Å]	19.360(3)	19.8187(7)	21.6090(16)	19.679(2)
c [Å]	24.058(3)	24.9006(8)	26.1005(18)	25.007(2)
β [°]	96.143(12)	94.083(2)	100.904(2)	93.795(7)
V [Å^3]	6970(2)	7366.0(4)	8321.0(10)	7409.6(12)
Z	4	4	4	4
$d_{calcd.}$ [g cm^{-3}]	1.054	1.127	1.315	1.417
μ [cm^{-1}]	2.33	11.54	39.58	53.64
2θ range [°]	2.1–55.0	2.6–52.8	2.4–58.0	4.4–50.0
Collected data	8286	169898	202037	13545
Unique data/*R*(int.)	7986/0.0185	15060/0.0918	22128/0.1642	13016/0.0841
Data with $I > 2\sigma(I)$ (N_o)	5553	9441	9870	5967
Parameters (N_p)	359	732	834	732
*R*1 [$I > 2\sigma(I)$][b]	0.0420	0.0446	0.0418	0.0416
*wR*2 (all data)[c]	0.1170	0.1305	0.1241	0.0881
GOF[d]	0.929	1.047	0.827	0.722
Largest diff. peak/hole [e Å^{-3}]	0.37/–0.26	0.95/–0.52	2.53/–1.44	1.07/–0.93

[a] All data were collected at 173 K by using Mo-K_α (λ = 0.71073 Å) radiation. [b] $R_1 = \Sigma(||F_o| - |F_c||)/\Sigma|F_o|$. [c] $wR2 = \{\Sigma[w(F_o^2 - F_c^2)^2]/\Sigma[w(F_o^2)^2]\}^{1/2}$. [d] $GOF = \{\Sigma[w(F_o^2 - F_c^2)^2]/(N_o - N_p)\}$.

Computational Methods: The Gaussian 03[31] package was used for all energy and frequency calculations. The energies of the model compounds were minimizedby using density functional theory with the functional MPW1B95,[32] starting from the crystallographically determined or from other derived geometries and assuming C_2 or D_2 symmetry for $\mathbf{2a_M}$ and $\mathbf{3a_M}$. An energy-consistent, quasi-relativistic pseudopotential of the Stuttgart/Cologne group with an optimized 12s12p8d3f valence basis set was employed for the heavier atom thallium (N = 60),[33a] where N denotes the number of core electrons. For the lighter atoms carbon, hydrogen, potassium, and sulfur the basis sets 6-31G* were used. For $\mathbf{4a_M}$, $\mathbf{4b_M}$, $\mathbf{5a_M}$, and $\mathbf{5b_M}$, frequency calculations were done to verify that the geometries are true minima on the potential-energy surface. The natural bond orbital analysis employed the Gaussian 03 adaptation of the NBO program.[33b] One part of the NBO program examines all possible interactions between filled (donor) Lewis-type NBOs and empty (acceptor) non-Lewis NBOs and estimates their energetic importance by second-order perturbation theory. The calculated perturbation energy $E^{(2)}$ corresponds to the associated stabilization by delocalization.

Supporting Information (see footnote on the first page of this article): Molecular structure plot of **2b**. Additional structural plots of **2a**, **2b**, **3a**, and **3b** showing views perpendicular and parallel to the central M_2E_2 rings. DFT-calculated structures of $\mathbf{2a_M}$, $\mathbf{3a_M}$, $\mathbf{4a_M}$, $\mathbf{4b_M}$, $\mathbf{5a_M}$, and $\mathbf{5b_M}$ with Cartesian coordinates. NBO charges for DFT-optimized $\mathbf{4a_M}$, $\mathbf{4b_M}$, $\mathbf{5a_M}$, and $\mathbf{5b_M}$.

Acknowledgments

Financial support by the Deutsche Forschungsgemeinschaft (DFG) within the framework program SPP 1166 is gratefully acknowledged.

[1] A. G. Lee, *The Chemistry of Thallium*, Elsevier, Amsterdam, **1971**.

[2] C. E. Housecroft, A. G. Sharpe, *Inorganic Chemistry*, 2nd ed., Pearson, Harlow, **2005**.

[3] J. B. A. Dumas, *Compt. Rend.* **1862**, *55*, 866–895.

[4] N. Wiberg, *Holleman-Wiberg – Lehrbuch der Anorganischen Chemie*, 102nd ed., de Gruyter, Berlin, **2007**.

[5] R. D. Shannon, *Acta Crystallogr., Sect. A* **1976**, *32*, 751–767.

[6] The Shannon ionic radius of Rb^+ (1.66 Å) is even closer to that of Tl^+. However, these radii were determined with strongly polarizing anions such as O^{2-} or F^- as counterions. Therefore, as was noted before in ref.[7], a comparison of the lattice constants of compounds with a less coordinating counteranion might be more suitable to illustrate the difference in the ionic radii, e.g., M_2PtCl_6 [$a(K_2PtCl_6)$ = 9.745 Å, $a(Rb_2PtCl_6)$ = 9.904 Å, and $a(Tl_2PtCl_6)$ = 9.775 Å].

[7] A.-V. Mudring, F. Rieger, *Inorg. Chem.* **2005**, *44*, 6240–6243.

[8] S. Basu, R. P. Rambo, J. Strauss-Soukup, J. H. Cate, A. R. Ferré-D′Amaré, S. A. Strobel, J. A. Doudna, *Nat. Struct. Biol.* **1998**, *5*, 986–992.

[9] M. L. Gill, S. A. Strobel, J. P. Loria, *J. Am. Chem. Soc.* **2005**, *127*, 16723–16732.

[10] For example, M_2SO_4. The halides MX (X = Cl, Br, I) crystallize in the rock salt (most stable for M = K) and cesium chloride (most stable for M = Tl) structure. In addition, TlF and yellow TlI adopt distorted forms of the sodium chloride structure. See: A. F. Wells, *Structural Inorganic Chemistry*, 5th ed., Clarendon Press, Oxford, **1984**.

[11] F. Wiesbrock, H. Schmidbaur, *J. Am. Chem. Soc.* **2003**, *125*, 3622–3630.

[12] a) C. Janiak, *Coord. Chem. Rev.* **1997**, *163*, 107–216; b) S. Schulz in *Comprehensive Organometallic Chemistry III* (Eds.: R. Crabtree, M. Mingos), Elsevier, Oxford, **2007**, vol. 3, chapter 7.

[13] M. Niemeyer, P. P. Power, *Angew. Chem. Int. Ed.* **1998**, *37*, 1277–1279.

[14] R. E. Dinnebier, U. Behrens, F. Olbrich, *Organometallics* **1997**, *16*, 3855–3858.

[15] a) F. Olbrich, U. Behrens, *Z. Kristallogr., New Cryst. Struct.* **1997**, *212*, 47; b) A. Dashti-Mommertz, B. Neumüller, S. Melle, D. Haase, W. Uhl, *Z. Anorg. Allg. Chem.* **1999**, *625*, 1828–1832.

[16] K. F. Tesh, T. P. Hanusa, J. C. Huffman, *Inorg. Chem.* **1990**, *29*, 1584–1586.

[17] K. W. Klinkhammer, S. Henkel, *J. Organomet. Chem.* **1994**, *480*, 167–171.

[18] E. Weiss, *Helv. Chim. Acta* **1963**, *46*, 2051–2054.

[19] L. F. Dahl, G. L. Davis, D. L. Wampler, R. West, *J. Inorg. Nucl. Chem.* **1962**, *24*, 357–363.

[20] P. Luger, C. André, R. Rudert, D. Zobel, A. Knöchel, A. Krause, *Acta Crystallogr., Sect. B* **1992**, *48*, 33–37.

[21] H. S. Lee, M. Niemeyer, *Inorg. Chem.* **2006**, *45*, 6126–6128.

[22] H. S. Lee, S.-O. Hauber, D. Vinduš, M. Niemeyer, *Inorg. Chem.* **2008**, *47*, 4401–4412.

[23] a) J. D. Smith, *Adv. Organomet. Chem.* **1999**, *43*, 267–348; b) K. Ruhlandt-Senge, K. W. Henderson, P. C. Andrews in *Comprehensive Organometallic Chemistry III* (Eds.: R. Crabtree, M. Mingos), Elsevier, Oxford, **2007**, vol. 2, chapter 1.

[24] a) M. Niemeyer, P. P. Power, *Inorg. Chem.* **1997**, *36*, 4688–4696; b) M. Niemeyer, P. P. Power, *Inorg. Chim. Acta* **1997**, *263*, 201–207.

[25] B. Krebs, A. Brömmelhaus, *Z. Anorg. Allg. Chem.* **1991**, *595*, 167–182.

[26] a) N. J. Hill, W. Levason, M. E. Light, G. Reid, *Chem. Commun.* **2003**, 110–111; b) H.-U. Hummel, E. Fischer, T. Fischer, D. Gruß, A. Franke, W. Dietzsch, *Chem. Ber.* **1992**, *125*, 1565–1570.

[27] For other compounds that show interactions between potassium cations and arene rings of Trip substituents, see ref.[24] and the following examples. Herein, the K···centroid distances fall in the range 2.74–3.19 Å: a) W. J. Grisby, P. P. Power, *J. Am. Chem. Soc.* **1996**, *118*, 7981–7988; b) L. Pu, A. D. Phillips, A. F. Richards, M. Stender, R. S. Simons, M. M. Olmstead, P. P. Power, *J. Am. Chem. Soc.* **2003**, *125*, 11626–11636.

[28] *Cambridge Structural Database*, London, UK, **2008**. For the search, the range of Tl···centroid–C angles was constrained to 85–95°, assuming only small ring slippage. For a larger ring slippage there appears to be no upper limit to the Tl···centroid distances.

[29] See for example, refs.[11] and: a) J. Beck, J. Strähle, *Z. Naturforsch.* **1986**, *41b*, 1381–1386; b) H. Schmidbaur, W. Bublak, J. Riede, G. Müller, *Angew. Chem. Int. Ed. Engl.* **1985**, *24*, 414–415; c) M. D. Noirot, O. P. Anderson, S. H. Strauss, *Inorg. Chem.* **1987**, *26*, 2216–2223; d) H. Schmidbaur, B. Bublak, B. Huber, J. Hofmann, G. Müller, *Chem. Ber.* **1989**, *122*, 265–270; e) S. D. Waezsada, T. Belgardt, M. Noltemeyer, H. W. Roesky, *Angew. Chem. Int. Ed. Engl.* **1994**, *33*, 1351–1352; f) W. Frank, G. Korrell, G. J. Reiß, *Z. Anorg. Allg. Chem.* **1995**, *621*, 765–770; g) W. Frank, G. Korrell, G. J. Reiß, *J. Organomet. Chem.* **1996**, *506*, 293–300; h) G. B. Deacon, E. E. Delbridge, C. M. Forsyth, B. W. Skelton, A. H. White, *J. Chem. Soc., Dalton Trans.* **2000**, 745–751; i) F. A. Kunrath, O. L. Casagrande Jr, L. Toupet, J.-F. Carpentier, *Eur. J. Inorg. Chem.* **2004**, 4803–4806; j) N. Oberbeckmann-Winter, P. Braunstein, R. Welter, *Organometallics* **2004**, *23*, 6311–6318; k) J. C. Thomas, J. C. Peters, *Polyhedron* **2004**, *23*, 2901–2913; l) H. V. R. Dias, S. Singh, T. R. Cundari, *Angew. Chem. Int. Ed.* **2005**, *44*, 4907–4910; m) K. Akhbari, A. Marsali, *J. Organomet. Chem.* **2007**, *692*, 5109–5112.

[30] H. Schmidbaur, A. Schier, *Organometallics* **2008**, *27*, 2361–2395.

[31] M. J. Frisch, G. W. Trucks, H. B. Schlegel, G. E. Scuseria, M. A. Robb, J. R. Cheeseman, J. A. Montgomery Jr, T. Vreven,

K. N. Kudin, J. C. Burant, J. M. Millam, S. S. Iyengar, J. Tomasi, V. Barone, B. Mennucci, M. Cossi, G. Scalmani, N. Rega, G. A. Petersson, H. Nakatsuji, M. Hada, M. Ehara, K. Toyota, R. Fukuda, J. Hasegawa, M. Ishida, T. Nakajima, Y. Honda, O. Kitao, H. Nakai, M. Klene, X. Li, J. E. Knox, H. P. Hratchian, J. B. Cross, C. Adamo, J. Jaramillo, R. Gomperts, R. E. Stratmann, O. Yazyev, A. J. Austin, R. Cammi, C. Pomelli, J. W. Ochterski, P. Y. Ayala, K. Morokuma, G. A. Voth, P. Salvador, J. J. Dannenberg, V. G. Zakrzewski, S. Dapprich, A. D. Daniels, M. C. Strain, O. Farkas, D. K. Malick, A. D. Rabuck, K. Raghavachari, J. B. Foresman, J. V. Ortiz, Q. Cui, A. G. Baboul, S. Clifford, J. Cioslowski, B. B. Stefanov, G. Liu, A. Liashenko, P. Piskorz, I. Komaromi, R. L. Martin, D. J. Fox, T. Keith, M. A. Al-Laham, C. Y. Peng, A. Nanayakkara, M. Challacombe, P. M. W. Gill, B. Johnson, W. Chen, M. W. Wong, C. Gonzalez, J. A. Pople, *Gaussian 03*, Revision D.01, Gaussian, Inc. Pittsburgh PA, **2003**.

[32] Y. Zhao, D. G. Truhlar, *J. Phys. Chem. A* **2004**, *108*, 6908–6918.

[33] a) T. Leininger, A. Berning, A. Nicklass, H. Stoll, H.-J. Werner, H.-J. Flad, *Chem. Phys.* **1997**, *217*, 19–27; b) E. D. Glendening, A. E. Reed, J. E. Carpenter, F. Weinhold, *NBO*, Version 3.1; c) K. B. Wiberg, *Tetrahedron* **1968**, *24*, 1083–1096.

[34] a) H. Hope, *Prog. Inorg. Chem.* **1994**, *41*, 1–19; b) G. M. Sheldrick, *SHELXTL PC 5.03*, Siemens Analytical X-ray Instruments Inc., Madison, WI, **1994**; c) G. M. Sheldrick, *SHELXL-97, Program for Crystal Structure Solution and Refinement*, University of Göttingen, **1997**.

Received: July 30, 2008
Published Online: November 12, 2008

